THE JOURNAL OF BIOLOGICAL CHEMISTRY VOL. 280, NO. 41, pp. 34974–34984, October 14, 2005

Rabphilin Localizes with the Cell Actin Cytoskeleton and Stimulates Association of Granules with F-actin Cross-linked by α-Actinin*

Received for publication, March 11, 2005, and in revised form, July 8, 2005 Published, JBC Papers in Press, July 25, 2005, DOI 10.1074/jbc.M502695200

Giovanna Baldini[‡], Alberto M. Martelli[§¶], Giovanna Tabellini[‖], Chad Horn[**], Khaled Machaca[‡‡], Paola Narducci[‡], and Giulia Baldini[1]**

*From the [‡]Dipartimento di Morfologia Umana Normale, via Manzoni 16, Trieste,Universita' di Trieste, Trieste I-34138, Italy, the [§]Dipartimento di Scienze Anatomiche Umane e Fisiopatologia dell'Apparato Locomotore, Sezione di Anatomia, Cell Signalling Laboratory, Universita' di Bologna, via Irnerio 48, Bologna I-40126, Italy, the [¶]Istituto per i Trapianti d'Organo e l'Immunocitologia del Consiglio Nazionale delle Ricerche, Sezione di Bologna c/o IOR, via di Barbiano 1/10, Bologna I-40136, Italy, the [‖]Dipartimento di Scienze Biomediche e Biotecnologie, Sezione di Citologia e Istologia, Università di Brescia, Viale Europa 11, Brescia I-25123, Italy, and the Departments of [‡‡]Physiology and Biophysics and of **Biochemistry and Molecular Biology, University of Arkansas for Medical Sciences, Little Rock, Arkansas 72205*

In endocrine cell, granules accumulate within an F-actin-rich region below the plasma membrane. The mechanisms involved in this process are largely unknown. Rabphilin is a cytosolic protein that is expressed in neurons and neuroendocrine cells and binds with high affinity to members of the Rab3 family of GTPases localized to synaptic vesicles and dense core granules. Rabphilin also interacts with α-actinin, a protein that cross-links F-actin into bundles and networks and associates with the granule membrane. Here we asked whether rabphilin, in addition to its granule localization, also interacts with the cell actin cytoskeleton. Immunofluorescence and immunoelectron microscopy show that rabphilin localizes to the sub-plasmalemmal actin cytoskeleton both in neuroendocrine and unspecialized cells. By using purified components, it is found that association of rabphilin with F-actin is dependent on added α-actinin. In an *in vitro* assay, granules, unlike endosomes or mitochondria, associate with F-actin cross-linked by α-actinin. Rabphilin is shown to stimulate this process. Rabphilin enhances by ~8-fold the granule ability to localize within regions of elevated concentration of cross-linked F-actin. These results suggest that rabphilin, by interacting with α-actinin, organizes the cell cytoskeleton to facilitate granule localization within F-actin-rich regions.

Rabphilin is a cytosolic protein expressed in neurons and endocrine cells that binds with high affinity to members of the Rab3 family of proteins, namely Rab3A, Rab3B, Rab3C, and Rab3D (for review see Ref. 1). Rab3 proteins and rabphilin are localized to synaptic vesicles and dense core granules (2–5). Rabphilin has a Rab3A binding domain at the amino terminus of the protein and two C2 domains that bind to phospholipids in a Ca^{2+}-dependent manner at the carboxyl terminus (6–9). Rabphilin localization on synaptic vesicles and granules suggest a role in regulated exocytosis of these vesicles. In PC12 cells, rabphilin overexpression increased by 30% regulated hormone secretion, whereas antisense expression of the protein decreases hormone release by 30% (10). Expression of rabphilin in insulin secreting cells enhanced by ~2-fold regulated release of insulin (11). These data indicate that rabphilin functions as a positive regulator of regulated exocytosis. *Caenorhabditis elegans* mutants with disrupted rabphilin function are severely lethargic in the absence of mechanical stimulation (12). Differently, mutant mice lacking rabphilin did not have obvious physiological impairments (13), indicating that other proteins can compensate for rabphilin function. Given the tight binding of rabphilin to members of the Rab3 family and the finding that both Rab3A and rabphilin dissociate from vesicles upon fusion (14), efforts have been spent to determine whether rabphilin and Rab3 effects on regulated granule release or synaptic transmission were related. However, the stimulatory effects of rabphilin on hormone release were independent of Rab3 function (15) and of association-dissociation cycles with membranes mediated by Rab3 (11). Inhibition of regulated exocytosis induced by Rab3 overexpression was also independent of a direct interaction with rabphilin (8). Both mice and *C. elegans* rabphilin mutants did not have the synaptic transmission defects generated by Rab3 mutants (13, 16). Therefore, Rabphilin may have functions that are not directly related to those of Rab3 and *vice versa*. Interestingly, neurons of mice lacking Rab3 proteins have less rabphilin than the controls. Moreover, in the mutant mice, targeting of Rabphilin to the synapse is impaired (13, 17). Thus, Rab3 function is important for rabphilin stability and targeting to the site of vesicle release. In addition to Rab3, rabphilin binds to another member of the Rab family of proteins, Rab27, which localizes to dense core granules and regulates hormone secretion (18–20). Rabphilin N terminus domain binds to α-actinin (21, 22), a component of the actin cytoskeleton that cross-links actin filaments (23) and localizes to granules (24, 25). In endocrine cells granules are specifically accumulated in an F-actin-rich region below the plasma membrane (26, 27). Starting from these data, we hypothesized that rabphilin binds to the actin cytoskeleton in an α-actinin-dependent manner and thereby facilitates granule interactions with F-actin networks.

EXPERIMENTAL PROCEDURES

Materials—Enzymes for DNA modification and restriction enzymes were purchased from Promega (Madison, WI). The pEGFP-C1 vector was purchased from Clontech (Palo Alto, CA). pcDNA3.1(+), pIND, and pVGRXR vectors along with Ponasterone A, hygromycin B, and Lipofectamine were purchased from Invitrogen. Mouse monoclonal

* This work was supported by National Institutes of Health Grant RO1-DK53293 and by the Arkansas Tobacco Settlement (to Giulia Baldini) and by an Associazione Italiana per la Ricerca sul Cancro grant (to A. M. M.). The costs of publication of this article were defrayed in part by the payment of page charges. This article must therefore be hereby marked "*advertisement*" in accordance with 18 U.S.C. Section 1734 solely to indicate this fact.

[1] To whom correspondence should be addressed: Dept. of Biochemistry and Molecular Biology, University of Arkansas for Medical Sciences, 4301 West Markham St., Slot 516, Little Rock, AR 72205. Tel.: 501-526-7793; Fax: 501-686-8169; E-mail: gbaldini@uams.edu.

IgG anti-rabphilin antibody (clone 47) was purchased from BD Transduction Laboratories; anti-Myc rabbit polyclonal and mouse monoclonal antibodies, anti-actinin rabbit polyclonal antibodies (H-300), and anti-Rab27a rabbit polyclonal antibodies (sc-22756) from Santa Cruz Biotechnology (Santa Cruz, CA); mouse monoclonal IgG anti-actin (clone MAB 1501) and anti-ACTH[2] antibodies from Chemicon International, Inc. (Temecula, CA); mouse monoclonal IgM anti-actin from Oncogene Research Products, Boston, MA; mouse monoclonal IgM anti-α-Actinin (clone BM-75.2), actin from bovine muscle, α-actinin from chicken gizzard, and retinoic acid from Sigma; peroxidase-conjugated streptavidin, mouse monoclonal antibodies anti-green fluorescent protein (GFP) and secondary peroxidase-conjugated anti-mouse IgG from Roche Applied Science; Texas Red-X-phalloidin, fluorescein isothiocyanate (FITC)-phalloidin, Alexa-fluor 568-conjugated actin from rabbit muscle, biotin-conjugated human transferrin, Antifade reagent (S-2828, component B), and MitoTracker Red CMXRos from Molecular Probes (Eugene, Oregon); FITC-conjugated anti-mouse IgG, Cy3-conjugated anti-mouse IgG, and rhodamine-conjugated anti-mouse IgM chain(μ chain specific) were from Jackson ImmunoResearch Laboratories, Inc. (West Grove, PA); FITC-conjugated anti-mouse (IgM specific) was from Sigma; anti-mouse IgG (γ-chain specific) conjugated to 5- or 10-nm gold particle and anti-mouse IgM chain (μ chain specific) conjugated to a 10-nm gold particle was from British BioCell International; enhanced chemiluminescence detection kits were purchased from PerkinElmer Life Sciences; recombinant Rab3A was purchased from Affinity BioReagents (Golden, CO); and mouse monoclonal anti-Rab3 antibodies (42.1) were purchased from Synaptic Systems (Goettingen, Germany).

Constructs—Rabphilin-pcDNA3 (11) was a kind gift from Dr. Pietro De Camilli (Yale University, New Haven). Rabphilin was amplified from rabphilin-pcDNA3 with primers 5′-CGG GGT ACC ACC ATG ACT GAC ACT GTG AAC and 5′-GCT CTA GAC TAG TCG CTC GAC ACG TG, cut with KpnI and XbaI and subcloned into vector pIND (Invitrogen). GFP obtained from vector pEGFP-C1 by digestion with NheI and KpnI was subcloned into the plasmid rabphilin-pIND cut with the same restriction enzymes to obtain GFP-rabphilin-pIND. The pIND plasmids were co-transfected with pVGRXR (Invitrogen), to achieve inducible expression of rabphilin and rabphilin-GFP. Murine POMC-pSP65 plasmid was a kind gift from Dr. Gary Thomas (Oregon Health Sciences University, Portland, Oregon). Pro-opiomelanocortin (POMC)-GFP was constructed using the following primers: 5′-AAAA-AAATTGCTAGCCACCATGCCGGAGATTCTGCTACAGT and 5′-AAAAAAATTTGCTAGCTTACCACCCTGGCCCTTCTTC-TGCG and performing PCR on POMC-pSP65. The product was digested with NheI and inserted into the pEGFP-C1 vector cut with NheI to obtain POMC-pEGFP. The Myc-Rab3A-pcB7 plasmid has been already described (4). Myc-tagged Rab3B in the pcDNA3 vector (Myc-Rab3B-pcDNA3) was a kind gift from Dr. Romano Regazzi (Université de Lausanne Lausanne, Switzerland). Rabphilin cDNA in the pGEX-2T vector was a kind gift from Dr. Ronald Holz (University of Michigan, Ann Arbor, MI) and Dr. I Macara (University of Virginia School of Medicine, Charlottesville).

Preparation of Post-nuclear Supernatants, Gel Electrophoresis, and Immunoblotting—Post-nuclear supernatants from untransfected PC12 cells and PC12 cells expressing Myc-Rab3B were prepared from 6-cm tissue culture dishes. Cells were scraped in 0.4 ml of homogenization buffer containing Tris-HCl, 10 mM, pH 7.4, EDTA 1 mM, and protein inhibitors (300 μg/ml phenylmethylsulfonyl fluoride, 1.5 μg/ml leupeptin, 6 μg/ml aprotinin, and 1.5 μg/ml pepstatin) and homogenized with 12 strokes in a 2-ml Teflon pestle homogenizer. The postnuclear supernatant was obtained by centrifugation of the homogenate at 600 × *g* for 5 min. Separation of proteins by SDS-PAGE, immunoblotting, with peroxidase-conjugated secondary antibodies, densitometry, and protein determination were all performed as described (28). Brain cytosol was prepared by homogenizing one rat brain in 10 ml of Kglu buffer (20 mM Hepes, pH 7.4, 120 mM potassium glutamate, 20 mM potassium acetate, 5 mM EGTA, 1 mg/ml bovine serum albumin). The homogenate was centrifuged at 95,000 rpm for 1 h in the TLA 100.2 rotor of the Beckman TLX centrifuge. The cytosol in the supernatant fraction was stored at −80 °C.

Actin Polymerization—G-actin was stored at a concentration of 16 μM in G buffer containing 0.2 mM ATP, 0.2 mM $CaCl_2$, 0.5 mM 2-mercaptoethanol, 0.5 mM NaN_3, 20 mM Tris-HCl, pH 8.0 (29). G-actin was polymerized for 1 h at 30 °C by adding one-tenth of the volume of 1 M KCl, 20 mM $MgCl_2$. Cross-linking was induced by addition of 1 μM α-actinin, and samples were further incubated for 1 h at 30 °C. To obtain Alexa-fluor 568-conjugated F-actin, Alexa-fluor 568-conjugated G-actin was polymerized as above and cross-linked by addition of 1 μM α-actinin.

Co-sedimentation of Rabphilin with F-actin—Recombinant glutathione S-transferase (GST) and rabphilin-GST were prepared by expression of pGEX-2T and pGEX-2T-rabphilin in *Escherichia coli* as previously described (30). Protein concentration was determined by using the BCA kit (Pierce). F-actin was incubated with and without 1 μM α-actinin in the presence or in the absence of different concentrations of rabphilin-GST for 1 h at 30 °C. Rabphilin binding to F-actin was determined by high speed co-sedimentation assay. Samples were centrifuged at 100,000 × *g* for 30 min to pellet polymerized actin (31). The pellets and supernatants were collected, and one-tenth of the samples were loaded onto a 10% SDS-PAGE and analyzed by Western blot with antibodies against actin (MAB 1501) and against rabphilin. For Rab3A, Rab27, and α-actinin pull-down experiments, rabphilin-GST and GST were kept bound to the glutathione-Sepharose 4B beads (Amersham Biosciences) used for protein purification.

Cell Culture and Transfections—Neuro2A (N2A) and COS-7 cells were cultured in DMEM with 10% fetal bovine serum and penicillin/streptomycin. To transiently express rabphilin subcloned into the inducible vector pIND, COS-7 cells and N2A cells were co-transfected with rabphilin-pIND and pVGRXR or GFP-rabphilin-pIND and pVGRXR using Lipofectamine 2000 according to the manufacturer (Invitrogen) instructions. Approximately 24 h after transfection, cells were trypsinized and plated on coverslips. After 5 h cells were induced with 5 μM Ponasterone A to induce expression of rabphilin. For some experiments, N2A cells were treated with retinoic acid (10 μM from a 1 mM stock in Me_2SO) for 10 h to induce neurite formation. N2A cell were transiently transfected with POMC-pEGFP or Myc-Rab3A-pcB7 (4) 48 h before experiments. PC12 cells were cultured in DMEM with 10% horse serum and 5% fetal bovine serum. PC12 cells were transfected with Myc-Rab3B-pcDNA3 with Lipofectamine. Stably transfected colonies expressing Myc-Rab3B were selected by growth in the presence of hygromycin B.

Preparation of Dense Core Granules Derived from N2A Cells—N2A cells (two 10-cm diameter tissue culture dishes) were washed twice with Kglu buffer and scraped from plates in the same buffer. Cells were broken in 0.4 ml of Kglu buffer by passing them five times through a 27.5-gauge syringe needle, and the post-nuclear supernatants were centri-

[2] The abbreviations used are: ACTH, adrenocorticotropic hormone; DMEM, Dulbecco's modified Eagle's medium; GFP, green fluorescent protein; GST, glutathione *S*-transferase; N2A, Neuro2A; POMC, pro-opiomelanocortin; FITC, fluorescein isothiocyanate; GTPγS, guanosine 5′-3-*O*-(thio)triphospate.

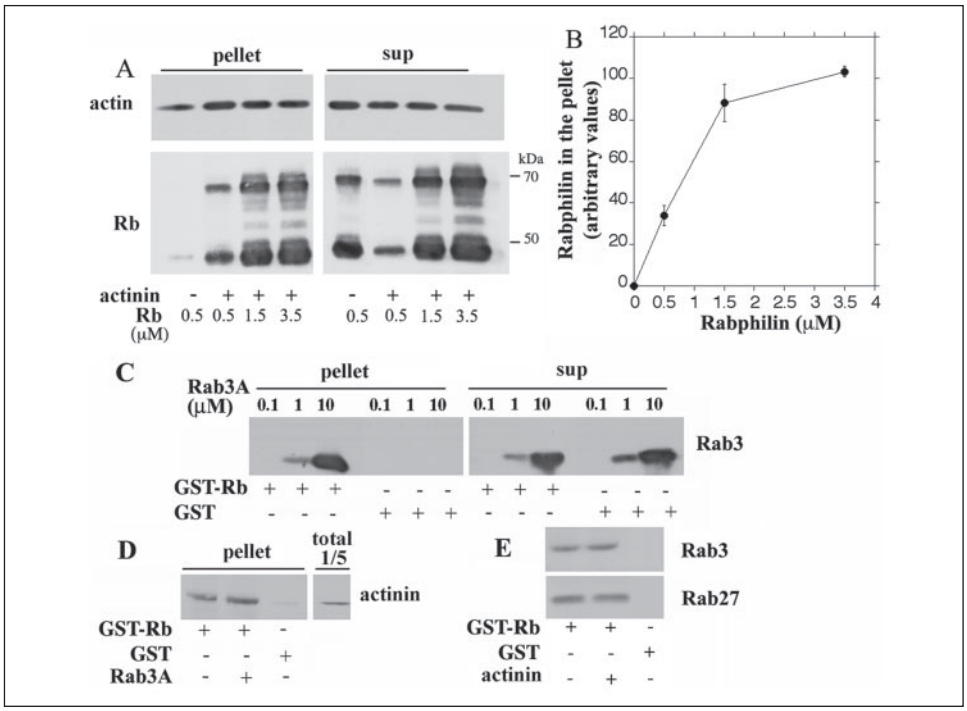

FIGURE 1. **Rabphilin binding to F-actin is dependent on α-actinin and is saturable.** *A*, G actin was polymerized to F-actin as described under "Experimental Procedures" and incubated with and without α-actinin (1 μM) or rabphilin at the indicated concentrations. Samples were centrifuged at 100,000 × *g* for 30 min. Samples (1/10 of total) were loaded onto a 10% SDS-PAGE gel. Western blot analysis was done with anti-rabphilin (*Rb*) and anti-actin (monoclonal antibody 1501, 1:5,000) monoclonal antibodies. *B*, the amount of rabphilin that co-sediments with actin in the pellet at different concentrations of total rabphilin added to the samples (band at 70 kDa) is shown in the graph. The data are the averages and standard deviations of three independent experiments, including the one shown in *panel A*. *C*, GST-rabphilin (GST-Rb) and GST immobilized onto Sepharose beads were incubated for 1 h at 4 °C with recombinant Rab3A at the indicated concentrations in A buffer (100 mM Tris-HCl, pH 7.4, 50 mM NaCl, 1 mM $MgCl_2$, 5 μM $ZnCl_2$, 1 mM dithiothreitol, and protease inhibitors) with 1 mM GTPγS. The beads were washed three times with A buffer with 0.5% Triton X-100. The beads were re-suspended in sample buffer and loaded onto a 10% SDS-PAGE gel. Western blot analysis was analyzed with anti-Rab3 antibodies. *D*, beads were incubated without and with 10 μM Rab3A, washed three times (as described in *panel C*), and then mixed with 1 μM α-actinin in A buffer. After incubation for 1 h at 4 °C, the beads were washed three times, loaded onto SDS-PAGE gel, and analyzed with antibodies (H-300) against α-actinin. *E*, beads were preincubated with 10 μM α-actinin and washed as in *panel D*. Beads were then incubated for 1 h at 4 °C with rat brain cytosol (4 mg/ml) in A buffer with 1 mM GTPγS, washed three times, and loaded onto the SDS-PAGE gel. The Western blot was probed with antibodies against Rab3 and Rab27. The experiments in *panels C–E* were done three times with similar results.

fuged at 7,200 × g for 10 min to obtain a pellet PII and a supernatant SII that contains cytosol and granule-containing fractions (32). SII was further centrifuged at 70,000 rpm for 30 min in the TLA 100.2 rotor of the Beckman TLX centrifuge to obtain the granule-containing pellet PIII and the supernatant SIII. Granules were re-suspended in GR buffer (0.1 ml) containing 100 mM KCl, 2 mM $MgCl_2$, 10 mM Hepes pH 7.4, 1 mM GTP, and 1 mM ATP. Re-suspended granules were further centrifuged at 7,200 × *g* for 10 min to eliminate aggregates. The granules (40 μl) were mixed with F-actin (0.1 ml) preincubated in the presence or in the absence of α-actinin (1 μM) and rabphilin (2 μM) at 30 °C for 1 h. The mixture was incubated at 30 °C for 30 min and centrifuged at 7,200 × *g* for 10 min. Co-sedimentation of granules with cross-linked actin was measured by Western blot analysis of the samples.

For experiments where endosomes were loaded with human biotin-conjugated transferrin, N2A cells were washed with DMEM three times and then incubated with biotin transferrin in DMEM (5 μg/ml). After 1 h incubation at 37 °C, cells were incubated for 2 min in a mild acidic buffer (120 mM NaCl, 20 mM NaCl, pH 5.0) and then washed twice with phosphate-buffered saline to release surface bound transferrin as described by others (33, 34). Biotin-conjugated transferrin in cell fractions was detected by Western blots analysis using peroxidase-labeled streptavidin.

Interaction of GFP-labeled Granules with Cross-linked F-actin—For experiments where the interaction of GFP-labeled granules with cross-linked F-actin was visualized by fluorescence microscopy, granules from N2A cells transiently expressing POMC-GFP (two 10-cm diameter tissue culture dishes) were obtained as described in the section above. Resuspended granules in GR buffer (40 μl) were mixed with Alexa-fluor-F-actin (0.1 ml) that was preincubated in the presence or in the absence of α-actinin (1 μM) and rabphilin (2 μM). After incubation at 30 °C for 1 h, 1 ml of Antifade reagent in phosphate-buffered saline was added to 20 μl of the samples to prevent sample photobleaching. The mixture was then transferred onto a glass slide, covered with a coverslip, and observed by fluorescence microscopy.

In Vivo Labeling of N2A Cell Mitochondria—N2A cells plated on coverslips were washed twice with DMEM and incubated with 200 nM MitoTracker (diluted from a 0.2 mM stock solution in Me_2SO). After 20-min incubation at 37 °C, cells were washed with DMEM twice and fixed for immunofluorescence with 3.7% formaldehyde solution in phosphate-buffered saline.

For the *in vitro* experiments where mitochondria were mixed with cross-linked F-actin, a crude cell fraction containing mitochondria labeled with MitoTracker (see below) was obtained from N2A post-nuclear supernatants as described (35). Briefly, the post-nuclear supernatant (0.4 ml) from a 10-cm plate incubated with 200 nM MitoTracker red as described above was centrifuged at 6,500 × *g* for 20 min in an Eppendorf microcentrifuge. Mitochondria in the pellet were re-suspended in 0.4 ml of GR buffer, and 40 μl of the mixture was added to cross-linked F-actin (100 μl). Samples were then incubated for 30 min at 30 °C. FITC-labeled phalloidin (1 μl) and Antifade reagent in phosphate-buffered saline (5 μl) were added to the mixture. Samples were

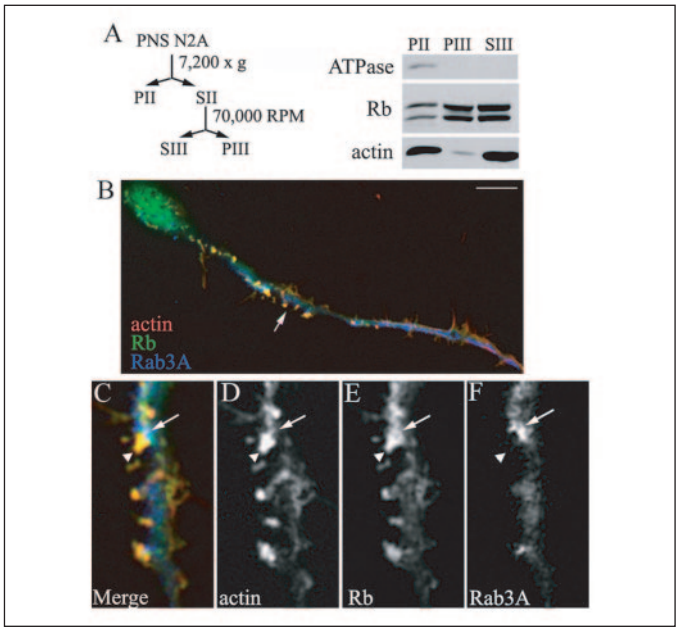

FIGURE 2. **Rabphilin-GFP co-localizes with F-actin in N2A cells.** *A*, post-nuclear supernatants derived from transfected N2A cells expressing GFP-rabphilin were centrifuged at 7,500 × *g* for 10 min to obtain a pellet PII and a supernatant SII. The supernatant SII was centrifuged at 70,000 rpm for 30 min in the Beckman 100.2 rotor to obtain a granule containing fraction (*PIII*) and a supernatant (*SIII*). Fraction PII (1/10 of total), PIII (1/2 of total), and SIII (1/10 of total) were loaded onto an SDS-PAGE gel, and Western blots were done with the indicated antibodies. *B–F*, transfected N2A cells expressing Myc-Rab3A and GFP-rabphilin were treated with retinoic acid to stimulate formation of neurite-like processes. F-actin (*red*) was stained with Texas-red-phalloidin. Myc-tagged Rab3A on granules (*blue*) was visualized by staining with anti-Myc rabbit polyclonal antibodies and Cy5-conjugated anti-rabbit antibodies. Cells were visualized by confocal microscopy.

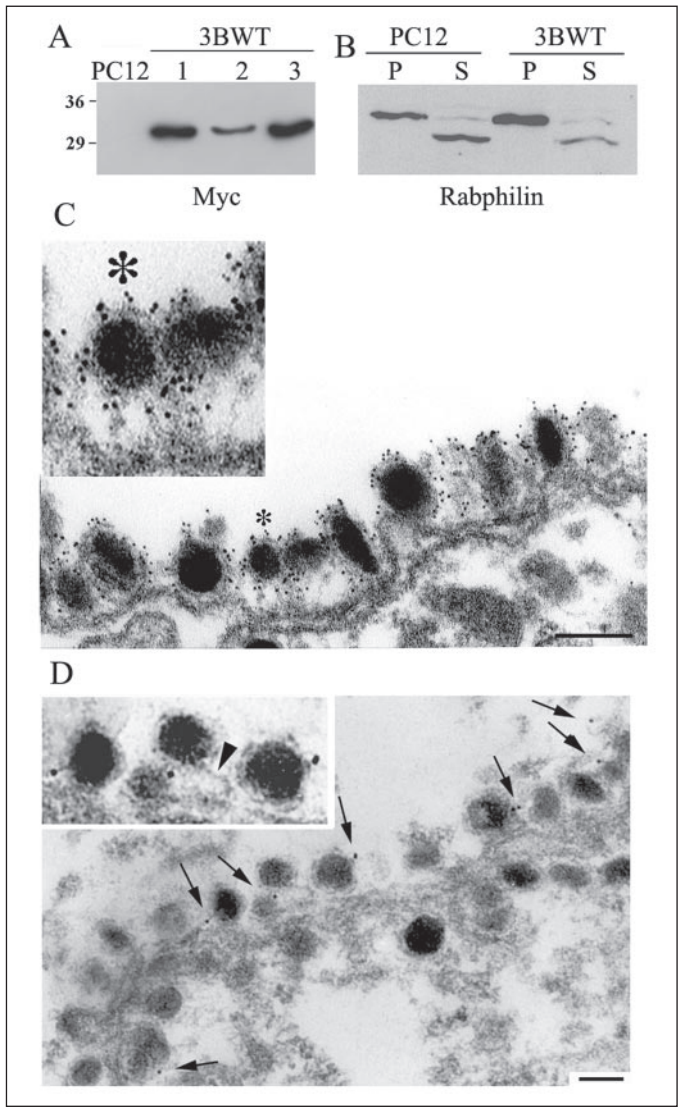

FIGURE 3. **Exogenous Rab3B and endogenous rabphilin localize to dense core granules morphologically docked to the plasma membrane.** *A*, PC12 post-nuclear supernatants of untransfected PC12 cells and PC12 cells stably expressing Myc-Rab3B (clone 3BWT1, clone 3BWT2, and clone 3BWT3) were loaded onto an SDS-PAGE gel. The Western blot was probed with mouse monoclonal antibodies against Myc to visualize Myc-tagged Rab3B. *B*, PC12 post-nuclear supernatants (0.4 ml) from untransfected PC12 cells and PC12 cells expressing Myc-Rab3B (clone 3BWT1) were centrifuged at 90,000 rpm for 1 h in the MLA-130 rotor of the Beckman TL Optima MAX-E centrifuge. The pellet was resuspended in 0.4 ml of homogenization buffer, and equal volumes of supernatant and pellet were loaded onto the SDS-PAGE gel. The Western blot was probed with monoclonal antibodies against rabphilin. *C*, Immunogold localization of broken PC12 cells expressing Myc-Rab3B. Samples were labeled with mouse monoclonal IgG against Myc, the secondary staining was done with 5 nm colloidal gold-conjugated anti-mouse IgG. *Bar*, 100 nm. The *inset* shows the region highlighted by the *asterisk* at a 2× magnification. *D*, samples were labeled with mouse monoclonal IgG against rabphilin, the secondary staining was done with 5 nm colloidal gold-conjugated anti-mouse IgG. *Arrows* in *B* indicate rabphilin staining on dense core granules; the *arrowhead* in the *inset* (2× magnification) indicates a filament tethering a granule to the plasma membrane.

transferred onto a glass slide, covered with a coverslip, and observed by fluorescence microscopy.

Immunofluorescence, Confocal Microscopy, and Immunoelectron Microscopy—Immunofluorescence staining was performed as described previously (28). Fluorescence microscopy was done using a 63× objective, on a Zeiss Axiophot fluorescence microscope. Confocal microscopy was performed with a Zeiss LSM 510 scanning laser confocal attachment mounted on a Zeiss Axiovert 100 TV inverted fluorescence microscope. Optical sections were 1-mm thick. Broken PC12 cells for immunoelectron microscopy were prepared for agarose embedding and immunoelectron microscopy as described (28). Granule and mitochondria interaction with F-actin structures generated by α-actinin were visualized by using an Olympus 1X71 inverted microscope equipped with argon laser (488 nm) and helium/neon laser (543 nm). Images were collected by using Photometrics CoolSnap HQ camera controlled by Metamorph. To measure clustering of granules within the actin structures, images of actin and granules were collected with the same exposure time (250 ms). Images were then analyzed using the "ImageJ" software program from the National Institutes of Health. Merged images were separated into the red (actin) and *green* (granule) components. Images of actin and granules were processed using 200 pixels as an arbitrary threshold. The thresholded images were combined in a new image, and the areas of granule clusters (in *black*) within areas of actin were measured and expressed as ratio granule area/actin area.

RESULTS

Rabphilin Binds to F-actin in an α-Actinin-dependent Manner—It is unknown whether the interaction of rabphilin with α-actinin (21) leads to an association of rabphilin with F-actin. To determine whether this is the case, we investigated whether rabphilin binds to F-actin by using an in vitro assay with purified actin cytoskeleton components. Polymerization of G-actin generates actin filaments that sediment after high speed centrifugation (100,000 × *g* for 30 min), whereas addition of α-actinin induces formation of bundles and networks of F-actin (36) that sediment at lower speed (10,000 × *g* for 10 min) (37). We reasoned that binding of rabphilin to actin filaments, whether or not cross-linked with α-actinin, would lead to co-sedimentation of rabphilin and actin in the

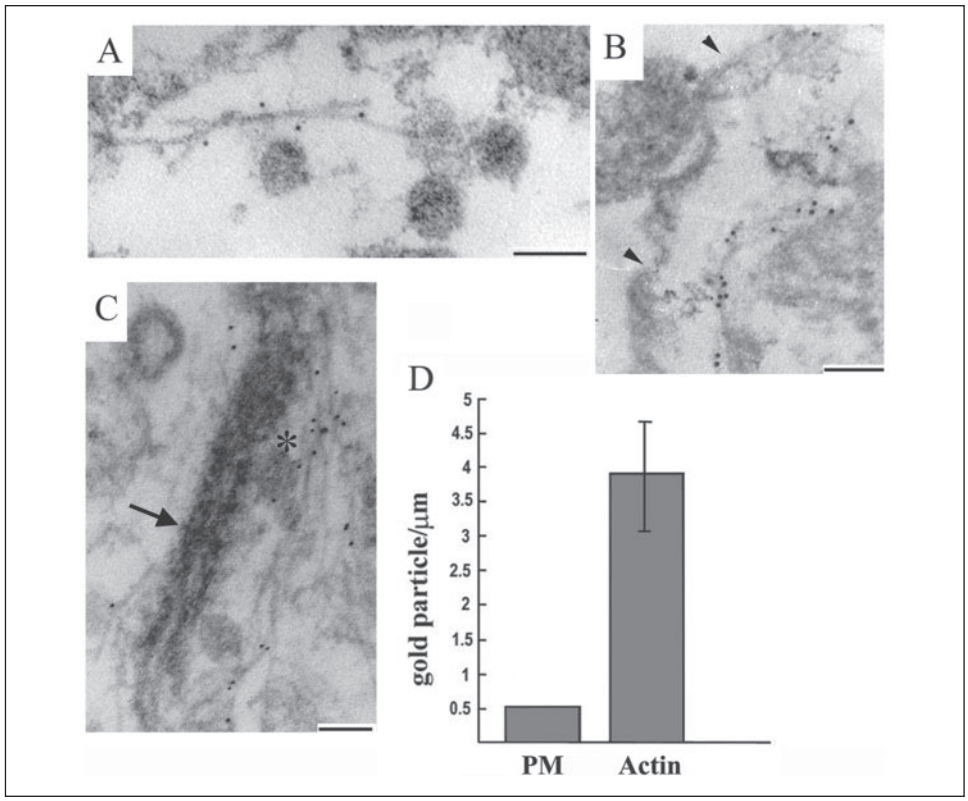

FIGURE 4. **Rabphilin associates with actin filaments in PC12 cells.** *A–C*, broken PC12 cells expressing Rab3B were labeled with mouse monoclonal IgG against rabphilin, the secondary staining was done with 5 nm colloidal gold-conjugated anti-mouse IgG. In *B* the plasma membrane is indicated by *arrowheads*. In *C* a cell junction is indicated by the *arrow*, and a granule by an *asterisk*. *Bar*, 100 nm. *D*, the graph shows the average number of rabphilin gold particle/μm and standard deviations. For the quantification, five images were obtained from four independent experiments. The criterion for choosing the image was the presence of detectable actin filaments and plasma membranes in the field. Data were collected by measuring the number of gold particles within 20 nm from either the plasma membrane (outer side) or the actin filaments (filament width = 5–10 nm). The total lengths of plasma membrane and filament examined were 9.39 μm and 11.4 μm, respectively.

pellet after centrifugation at high speed. G-actin was first incubated in polymerization conditions to make F-actin and then further incubated in the presence of rabphilin with or without α-actinin. In the absence of α-actinin, after the high speed centrifugation step, ~30% of the total actin in the sample was found in the pellet (Fig. 1). This indicates that a fraction of G-actin has polymerized into filaments in our experimental conditions. Recombinant GST-rabphilin appeared in the Western blot as two major bands of ~70 kDa and 50 kDa, as described by others (30). Only a small fraction (<5%) of total rabphilin in the sample was found to co-sediment with F-actin. Thus, rabphilin does not bind directly to actin filaments. Addition of α-actinin increased the amount of actin in the pellet and induced co-sedimentation of rabphilin (60% of total) with actin. This indicates that rabphilin binds to F-actin in an α-actinin-dependent manner. Binding of rabphilin to F-actin saturates at ~1.5 μM (Fig. 1*B*).

In addition to α-actinin, rabphilin binds to activated, GTP-bound Rab3A, and Rab27 (7, 14, 20, 38). It has been proposed that Rab3A inhibits binding of rabphilin to α-actinin (21). We investigated this possibility by *in vitro* pull-down experiments using GST-rabphilin immobilized onto glutathione-Sepharose beads. Recombinant GTPγS-Rab3A bound to GST-rabphilin and not to GST immobilized onto the Sepharose beads (Fig. 1*C*). This shows that the commercial recombinant Rab3A preparation used in this study binds to rabphilin. When beads with GST-rabphilin or with GST-rabphilin-Rab3A were mixed with α-actinin, the same amount of α-actinin was pulled down (Fig. 1*D*). This indicates that both rabphilin and rabphilin-Rab3A bind to α-actinin. It has been shown that Rab3 and Rab27 bind to rabphilin (1, 39). In agreement with this, GST-rabphilin on the beads pulled down both Rab3 and Rab27 from brain cytosol. α-Actinin did not inhibit binding of either Rab3A or Rab27 to GST-rabphilin (Fig. 1*E*). In conclusion, these data suggest that the binding of rabphilin to Rab3A (or Rab27) and to α-actinin is not mutually exclusive.

Rabphilin Localizes Both to the Actin Cell Cytoskeleton and to the Granules—The experiments described above suggest that rabphilin may bind to the cell actin cytoskeleton in addition to its established localizations in the cytosol and on the surface of dense core granules or synaptic vesicle (10, 14, 15, 30, 40). However, rabphilin localization to cell actin filaments has not been described. Neuroendocrine N2A cells (41) do not express endogenous rabphilin (not shown). In transfected N2A cells, rabphilin-GFP appeared as a doublet of ~100 kDa (Fig. 2A). Most of the cell rabphilin (~60%) was recovered in the supernatant (SIII) after high speed centrifugation (70,000 rpm), indicating its cytosolic localization. A fraction of cell rabphilin (20%) was found in the pellet PIII that also contains dense core granules (32). Another fraction of cell rabphilin was found in a low speed pellet (PII) where most of the plasma membrane marker Na^+/K^+-ATPase and 50% of the cell actin were also recovered. To determine whether rabphilin localized to the actin cytoskeleton, N2A cells transiently expressing Myc-tagged Rab3A were incubated with 10 μM retinoic acid (42). In these conditions, 30% of N2A cells formed neurite-like processes that were at least 3-fold longer than the cell body. We have shown that endogenous and Myc-tagged Rab3A localizes to dense core granules (4, 28). In the N2A cells, Rab3A fluorescence appeared as discrete puncta concentrated in the cell neurite processes, consistent with Rab3A granule localization. At the neurite margins there were spots of F-actin accumulation where Rab3A-labeled granules were excluded (Fig. 2, *C–F*, *arrowheads*). Differently, rabphilin-GFP co-localized with F-actin at these spots. Rabphilin staining was also concentrated at zones with less F-actin that had accumulated granules (Fig. 2, *C–F*, *arrows*), consistent with the established localization of the protein to the vesicle membrane (10, 15, 30). The co-localization of rabphilin and F-actin in the absence of granules was visible in virtually all the neurite-like processes examined (30 cells, 3 independent experiments). These data indicate that exogenous rabphilin associates both to actin filaments and granules in the N2A cells.

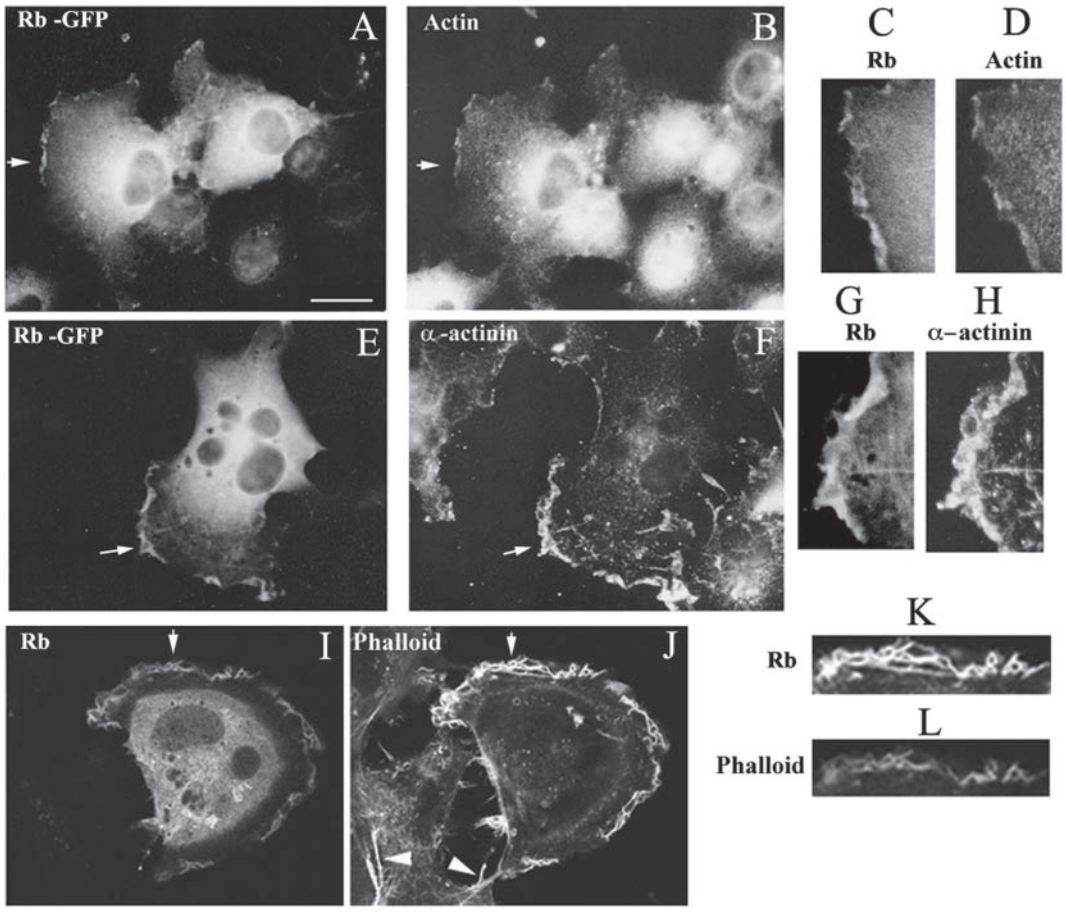

FIGURE 5. **Rabphilin localizes to the actin cytoskeleton in COS-7 cells.** *A–D*, immunofluorescence analysis of COS-7 cells transiently expressing rabphilin-GFP (Rb-GFP). Cells were stained with mouse monoclonal (IgM) antibodies against actin and with rhodamine-conjugated anti-mouse IgM. *E–H*, immunofluorescence analysis of COS-7 cell expressing rabphilin-GFP stained with antibodies against α-actinin and with rhodamine-conjugated anti-mouse IgM. *I–L*, confocal immunofluorescence of COS-7 cells transiently expressing exogenous rabphilin. Cells were labeled with mouse monoclonal antibody against rabphilin (*Rb*) and with FITC-conjugated donkey anti-mouse IgG, F-actin was stained with Texas red-phalloidin. Regions at the *arrows* are shown at higher magnification (2×) in *C*, *D*, *G*, *H*, *K*, and *L*.

To determine the cell distribution of endogenous rabphilin, we used undifferentiated PC12 cells where granules are accumulated at the cell cortex (4, 27, 43). Because of the close spatial relationship of plasma membrane, granules, and actin network in PC12 cells, we analyzed rabphilin distribution by immunoelectron microscopy. It has been reported that expression of exogenous Rab3B in PC12 cells reorganizes the actin cytoskeleton with induction of filopodia (44) and increases the amount of rabphilin associated with the particulate cell fraction (45). In agreement with these data, the amount of endogenous rabphilin found in a high speed centrifugation pellet was higher when cell homogenates were derived from PC12 cells stably expressing exogenous Rab3B than from the control cells (Fig. 3, *A* and *B*). Thus, PC12 cells overexpressing Rab3B may have more actin cytoskeleton and associated rabphilin than parental PC12 cells and were therefore chosen for ultrastructural analysis. Immunoelectron microscopy showed that Rab3B is associated to granules docked to the plasma membrane (Fig. 3*C*) in agreement with another report (45) and as previously shown also for Rab3A, Rab3D, and Rab3C (3, 4, 28, 45). Rabphilin immunogold labeling was found on ~30% of the granule docked to the plasma membrane (200 docked granules examined, 2 independent experiments). Granules did not have associated gold particles when the staining was done only with the secondary antibody. Thus, granules positioned at the cell cortex have both Rab3 and rabphilin associated to their surface. A fraction of docked granules (at least 5%, 300 granules observed) were linked to the plasma membrane by filaments (Fig. 3*D*, *arrowhead*).

Rabphilin, in addition to its granule localization, was associated to thin filaments of 5- to 10-nm diameter in the proximity of the plasma membrane (Fig. 4). Rabphilin staining on the filaments, as well as that on the granules, is specific, because almost no staining was detected on the outer surface of the plasma membrane (Fig. 4, *B–D*) or on mitochondria (not shown). Thus, immunoelectron microscopy shows that endogenous rabphilin associates to the actin cytoskeleton in PC12 cells overexpressing Rab3B.

In transfected COS-7 cells, exogenous rabphilin and rabphilin-GFP had a diffuse fluorescence distribution that was concentrated at the cell body (Fig. 5), consistent with the finding that >50% of the protein is in the cytosol (data not shown). Rabphilin co-localization with F-actin and with α-actinin and was found at the margins of flat processes (arrows). The co-localization of rabphilin with F-actin or α-actinin was detectable in ~25% of the rabphilin-transfected cells (100 cells examined). This indicates that rabphilin binds to the actin cytoskeleton in unspecialized cells.

Rabphilin Stimulates in Vitro Granule Association to F-actin Cross-linked by α-Actinin—Endocrine cells maintain a population of granules embedded within the F-actin network the cell cortex (26, 27, 46). Because rabphilin binds to α-actinin/F-actin, these interactions may

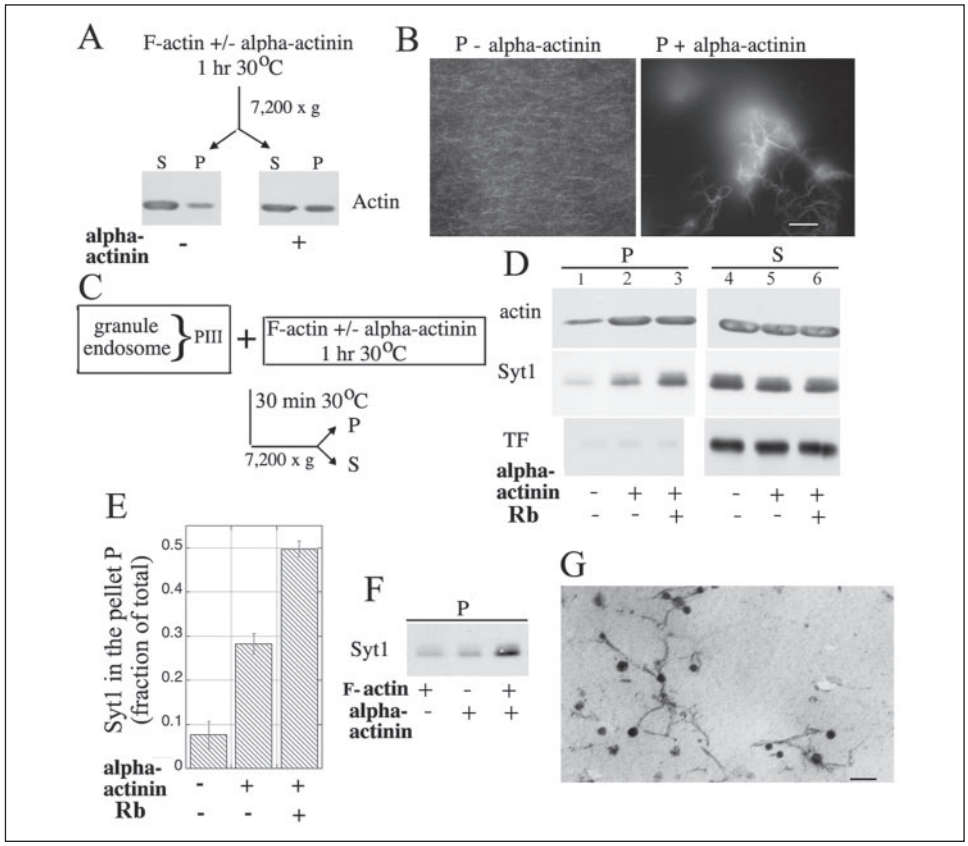

FIGURE 6. **Rabphilin stimulates granule, but not endosome, association to F-actin cross-linked by α-actinin.** *A*, F-actin (0.1 ml) was incubated in the absence and in the presence of α-actinin and centrifuged at 7200 × *g* for 10 min. Pellets were analyzed by Western blot. *B*, F-actin incubated in the presence or in the absence of α-actinin as above was further incubated with FITC-phalloidin for 10 min at room temperature. After the centrifugation step, the pellet was re-suspended in 20 μl of a solution containing 100 mM KCl and 2 mM $MgCl_2$ and observed by fluorescence microscopy. *C*, outline of the experimental procedure to study granule/endosome interaction with F-actin. *D*, N2A cells were incubated with biotin-transferrin (5 μg/ml) to label endosomes. Granules and transferrin-labeled endosomes in PIII (PIII was obtained as in Fig. 2*A* were re-suspended and mixed with F-actin preincubated in the absence and in the presence of 1 μM α-actinin and 2 μM rabphilin (*Rb*). The pellet (*P*) and supernatant (*S*) samples, obtained as described in *panel C*, were loaded onto a 10% SDS-PAGE gel. The Western blot analysis was done with antibodies against actin and synaptotagmin 1 (*Syt1*). Biotin-transferrin (*TF*) was visualized by probing the blot with peroxidase-conjugated streptavidin. *E*, the graph shows the fraction of total synaptotagmin 1 (*Syt1*) in the samples, which co-sedimented with actin in the *pellet P*. The data are averages and standard deviations of three independent experiments, including the one shown in *panel D*. *F*, granules derived from re-suspended PIII fraction were incubated with or without F-actin and α-actinin, as indicated. The *pellet P* was obtained as in *panel C*. Samples were analyzed by Western blot with anti-synaptotagmin 1 (*Syt1*) antibodies. *G*, the *pellet P* (obtained as in *panel C*) from samples where granules were incubated in the presence of F-actin and α-actinin was included in agarose and processed for electron microscopy (*bar* = 100 nm).

promote granule localization within cross-linked actin filament networks. To explore this possibility, we used an in vitro system where granules were added to F-actin cross-linked by α-actinin in the presence or in the absence of rabphilin. As described by others (37), addition of α-actinin to F-actin leads to the formation of large structures of cross-linked actin polymers that sediment after low speed centrifugation (Fig. 6, *A* and *B*). We reasoned that granule interaction with these structures would lead to co-sedimentation of the vesicles with cross-linked F-actin. To determine whether this is the case, we asked whether Synaptotagmin 1 (Syt1), a component of the granule membrane, co-sediments with cross-linked F-actin. We also predicted that, if the interactions of granules with cross-linked F-actin were specific, then other organelles would not co-sediment with the F-actin aggregates. For these experiments, we used N2A cells where endosomes were loaded with biotin-transferrin. After centrifugation of the granule-containing supernatant SII at high speed (70,000 rpm, see Fig. 2*A*), both Syt1, a component of the granule membrane, and a fraction of endocytosed biotin-transferrin were recovered in the pellet PIII (not shown). Thus, PIII contains both granules and transferrin-labeled endosomes. When the re-suspended pellet PIII was incubated with cross-linked actin and re-centrifuged at low speed, a fraction (~30% of total) of Syt1 was found in the pellet P (Fig. 6, *D* and *E*), indicating that granules associate to the actin structures generated by α-actinin. When granules were added to a sample containing α-actinin, but not F-actin, the amount of granules in the pellet P was the same as in control samples with granules, F-actin, but no α-actinin (Fig. 6*F*). This shows that sedimentation of granules after low speed centrifugation is not the result of α-actinin-induced aggregation of the vesicles. Unlike Syt1, biotin-transferrin remained in the supernatant S whether or not actin filaments were cross-linked by α-actinin (Fig. 6*D*). This

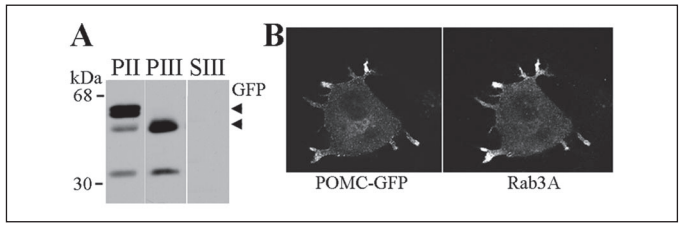

FIGURE 7. **POMC-GFP is processed and targeted to granules.** *A*, post-nuclear supernatants of N2A cells transiently transfected with POMC-pEGFP were centrifuged as described in *panel A* of Fig. 2. Fraction PII (one-tenth of total sample) and PIII (one-half of total sample) were analyzed by Western blot with antibodies against GFP. The bands indicated at the *arrows* were also detected by anti-ACTH antibodies. *B*, confocal fluorescence microscopy of N2A cells co-transfected with POMC-GFP-pEGFP and with Myc-Rab3A-pcB7. Fixed cells were stained with rabbit polyclonal antibodies against Myc and with Cy3-conjugated anti-rabbit IgG.

indicates that the population of endosomes in PIII, unlike the granules, did not associate with the cross-linked F-actin structures. Thus, co-sedimentation of granules with the actin aggregates generated by α-actinin is specific for these vesicles. Electron microscopy of pellets containing granules and cross-linked actin (Fig. 6*G*) showed that >90% of granules (100 granules observed from 3 independent experiments) were found in the proximity (within 50 nm) of actin filaments, rather then distributed randomly. This indicates that granules co-sediment at low speed with the F-actin aggregates generated by α-actinin, because they bind to the filaments. Rabphilin (2 μM) induced an 80% increase of granule association with cross-linked actin as compared with similar samples treated without rabphilin (Fig. 6, *D* and *E*). Conversely, addition of rabphilin did not increase the amount of actin recovered in the pellet after centrifugation. Thus, the increased association of granules with

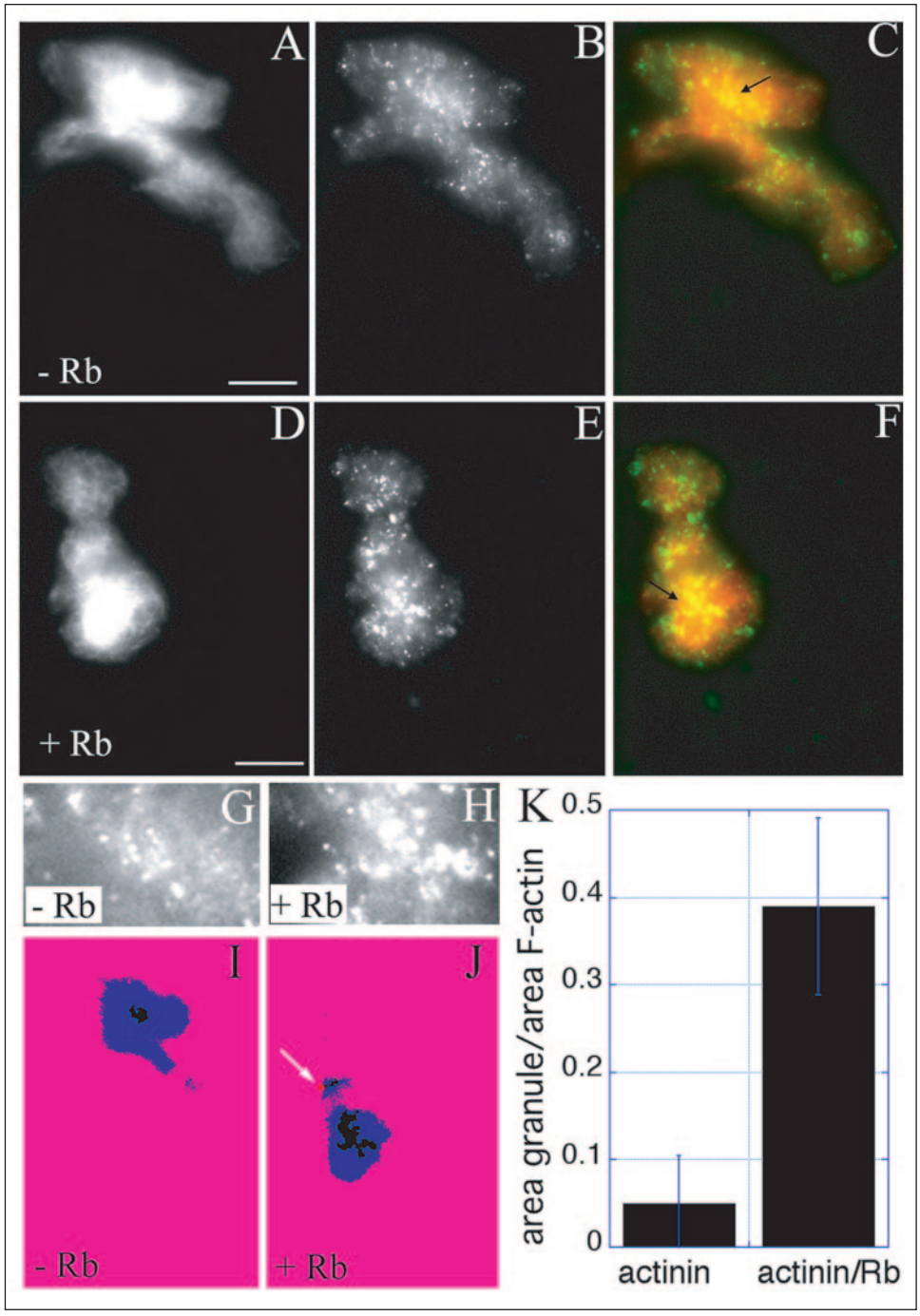

FIGURE 8. **Rabphilin induces *in vitro* clustering of granules within regions of elevated actin concentration.** *A–F*, granules derived from cells expressing POMC-GFP were incubated with Alexafluor 568-conjugated F-actin cross-linked by α-actinin in the absence (*A–C*) and in the presence (*D–F*) of 2 μM rabphilin (*Rb*). Samples were directly visualized by fluorescence microscopy. Actin (*red fluorescence*, *A* and *D*), granules (*green fluorescence*, *B* and *E*), and merged images (*C* and *F*) are shown. *Bars* in *A* and *D*, 10 μm. *G* and *H*, the regions indicated by the *arrows* in the *merged images* (*C* and *F*) are shown at a 3× magnification (granules, *green fluorescence*) in *G* and *H*, respectively. *I–J*, *merged images* shown in *C* and *F* were split into the *red* (actin) and *green* (granule) channels, thresholded, and merged again together as described under "Experimental Procedures" by using the Image J program from the National Institutes of Health. The areas of F-actin at elevated concentration are represented in *blue*. The areas of granule accumulation that do or do not overlap with F-actin at elevated concentration are represented in *black* and in *red* (*arrow*), respectively. *K*, the ratio, area of granule accumulation (in *black*, *panels I* and *J*):area of F-actin at elevated concentration (in *blue*, *panels I* and *J*), was derived from six thresholded images from three independent experiments. Data in the graph are expressed as averages and standard deviations. The total areas of cross-linked F-actin at elevated concentration analyzed for these experiments were 488 and 424 μm^2 for samples treated with and without rabphilin, respectively.

F-actin in the presence of rabphilin is not dependent upon an increased number or size of the actin aggregates in the pellet, but rather reflects an increased efficiency of granule interaction with the cross-linked F-actin.

The co-sedimentation experiments described above together with the electron microscopy analysis of the granules and actin filaments in the low speed pellets indicate that granules bind to F-actin cross-linked by α-actinin. To visualize by fluorescence microscopy binding of granules to F-actin cross-linked by α-actinin, we created a GFP-tagged hormone that localizes to dense core granules. When N2A cells express the exogenous ACTH precursor pro-opiomelanocortin (POMC), the precursor is converted to active hormones that are stored in granules and released in a regulated manner (41). To target GFP to the granules, N2A cells were transiently transfected with a plasmid, POMC-pEGFP, containing the cDNA of POMC linked to GFP. Transfected cells expressed a 61-kDa protein (Fig. 7*A*) that was detected with both anti-ACTH and anti-GFP antibodies and therefore corresponds to a fusion protein containing POMC (31 kDa) and GFP (30 kDa). In the transfected cells, another 48-kDa band was detected with both anti-ACTH and anti-GFP antibodies, indicating that POMC-GFP is cleaved to a smaller peptide. Unlike the 61-kDa POMC-GFP, most of the 48-kDa peptide fractionated with the granule-containing fraction PIII (32). In N2A cells transfected with POMC-GFP, the GFP fluorescence accumulated at the tips of the processes where it co-localized with overexpressed Rab3A (Fig. 7*B*) that is associated to the granule membrane (4). In conclusion, the data show that POMC-GFP precursor is processed to a cleaved product that is targeted to granules.

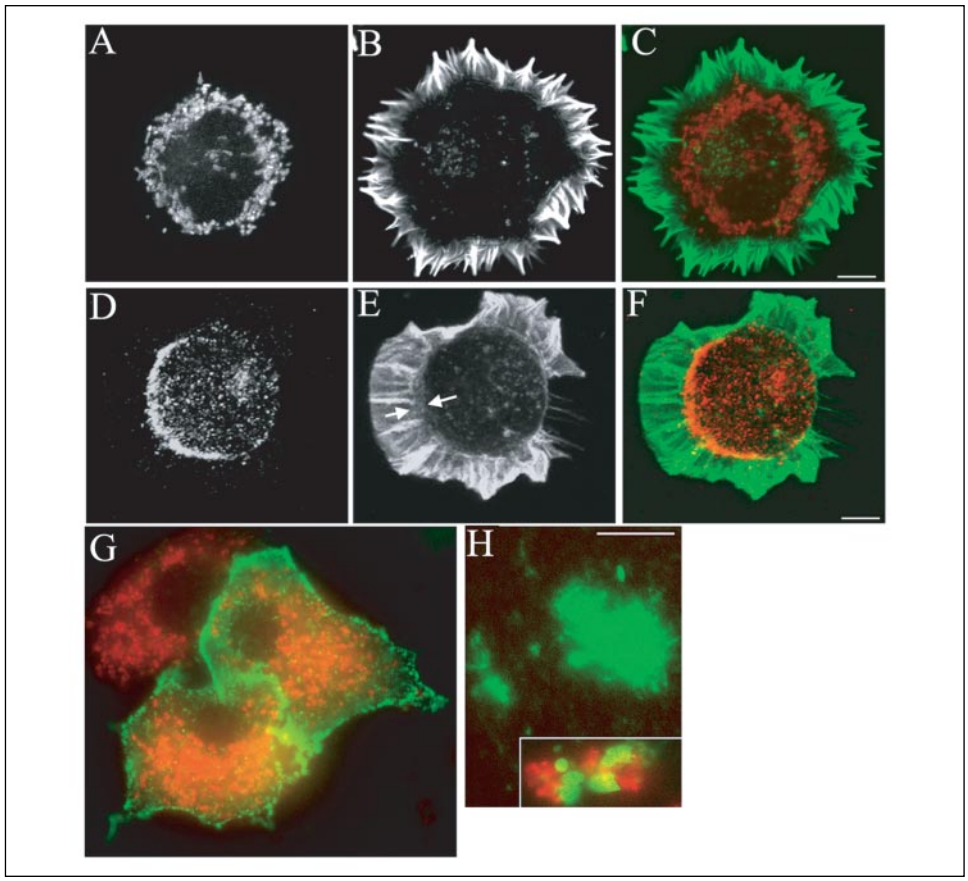

FIGURE 9. **Mitochondria do not associate to F-actin aggregates generated by α-actinin.** *A–C*, distribution of mitochondria and F-actin in N2A cells by confocal microscopy. Mitochondria were labeled with MitoTracker (*A*), and F-actin was stained with FITC-phalloidin (*B*), merged image (*C*). *D–F*, distribution of granules and F-actin in N2A cells by confocal microscopy. Granules were visualized by staining with anti-Rab3A mouse monoclonal antibodies and with Cy3-conjugated anti-mouse antibodies (*D*); F-actin was stained with FITC-phalloidin (*E*), the *double arrow* indicates a zone of F-actin and granule accumulation below the filopodia; the merged image is in *F*. *G*, fluorescence microscopy of PC12 cells transfected with Myc-Rab3A. Granules were visualized by staining with anti-Myc rabbit polyclonal antibodies and FITC-conjugated anti-rabbit secondary antibodies. Mitochondria were labeled with MitoTracker. *H*, F-actin cross-linked by α-actinin and MitoTracker-labeled mitochondria derived from N2A cells were mixed and observed by fluorescence microscopy as described under "Experimental Procedures." *Bars*, 10 μm.

When granules labeled with POMC-GFP were mixed with cross-linked actin, they appeared as fluorescent puncta co-localized with the cross-linked structures created by α-actinin (Fig. 8, *A–C*). These experiments show that POMC-GFP-labeled granules bind to the cross-linked actin structures created by α-actinin. In the presence of rabphilin, granules formed larger accumulations within zones of elevated actin concentration (Fig. 8, *D–F*, and, at higher magnification, *G* and *H*). Rabphilin increased the area of granules clustered ~8-fold within zones of concentrated actin as compared with control samples without the protein (Fig. 8, *I–K*).

In PC12 cells, granules are embedded in an actin-rich region below the plasma membrane (27, 43). Similarly, in round N2A cells, granules are accumulated in a cortical actin-rich region at the base of numerous filopodia (Fig. 9, *D–F*). Both in N2A and PC12 cells (Fig. 9*G*) mitochondria are more centrally located than the granules. We reasoned that, if the granule association to cross-linked actin observed *in vitro* is specific for these organelles, then mitochondria may be excluded from these structures. To determine whether this is the case, mitochondria derived from cells labeled with MitoTracker were mixed with cross-linked actin *in vitro* and observed by fluorescence microscopy. The actin aggregates did not have co-localized mitochondria (Fig. 9*H*). When cross-linked actin and mitochondria were found in close vicinity, there was virtually no overlap of the mitochondria and F-actin fluorescence (Fig. 9*H*, *inset*). Thus, mitochondria, unlike granules, are excluded from F-actin networks generated by α-actinin.

DISCUSSION

Rabphilin binds α-actinin (21), a cell cytoskeleton component that cross-links F-actin into bundles and networks. Here, we have extended this observation by showing that *in vitro* binding of rabphilin to α-actinin leads to its association with F-actin. This observation prompted us to further study rabphilin distribution in endocrine cells where the protein localizes to dense core granules and to the cytosol (10, 15, 30). Immunofluorescence localization of rabphilin to the actin cytoskeleton in round endocrine cells is difficult to determine, because granules with rabphilin on their surface are embedded in the cortical actin network (27, 46). Therefore, we induced N2A cells to extend long neurites where by confocal microscopy we could discriminate between zones of F-actin and granule accumulation at the margins of the processes. By using this approach we found that exogenous rabphilin co-localizes with zones of F-actin that do not have granules. Immunoelectron microscopy of broken PC12 shows that endogenous rabphilin localizes to F-actin and to the granule membrane. In conclusion it is found that rabphilin associates to the actin cytoskeleton in addition to its established localization to the granule surface and in the cytosol.

It has been reported that α-actinin, in addition to cross-linked F-actin, binds to the membrane of dense core granule membrane (24, 25). It is possible that rabphilin/α-actinin association facilitates granule binding to networks of F-actin created by α-actinin. To explore this possibility, we used an *in vitro* approach with purified cytoskeleton components. Co-sedimentation, electron microscopy and immunofluorescence assays show that granules, but not endosomes or mitochondria, associate to cross-linked actin structures generated by α-actinin *in vitro*. When cross-linked F-actin networks were formed in the presence of rabphilin, more granules associated with these structures and granules co-localized more efficiently with zones of elevated F-actin concentration. On the basis of these data, it is concluded that granules bind specifically to F-actin cross-linked by α-actinin and that rabphilin stimulates these interactions. It is possible that α-actinin, which exists as a divalent homodimer (23), may bind on one end to the granule membrane and

with the other end to the actin filament. This function of α-actinin as a connection between the granule membrane and F-actin may be similar to other activities of α-actinin, such as anchoring actin filaments to the plasma membrane (47, 48). In agreement with data from other groups, we find that rabphilin binds both to Rab3A and Rab27 (reviewed in Refs. 1 and 39). Differently from another report (21), we found that Rab3A did not inhibit the interaction of rabphilin with α-actinin *in vitro*, nor did α-actinin inhibit Rab3A or Rab27 binding to rabphilin. Thus, our data support a model whereby activated Rab3A or Rab27 on the granule membrane bind to both rabphilin and α-actinin. Such complexes could function to connect the granule to the cortical actin cytoskeleton. In agreement with this, we have found that increased Rab3A on the granule surface enhances their positioning at the cell cortex in PC12 cells (4). It is also possible that α-actinin binds to components of the granule membrane other than rabphilin/Rab3A.

In endocrine cells almost all F-actin is localized below the plasma membrane and organized in a tight mesh that was classically proposed to hinder granule access to the plasma membrane. However, more recently, data from many reports have suggested that cortical actin has a dual role in regulated exocytosis, because it may both hinder and mediate the movements of the granules (reviewed in Ref. 49). For example, it has been proposed that active Cdc42, while increasing cortical actin, also stimulates regulated granule release by PC12 cells (50). Our *in vitro* experiments show that α-actinin connects granules to F-actin and that this activity is stimulated by rabphilin. In endocrine cells such interactions may lead to enhanced α-actinin-dependent clustering of granules at the cortical region. Stimulation of exocytosis and consequent re-organization of the actin cytoskeleton may induce more granules to be released in close proximity of the plasma membrane, thereby enhancing their ability to dock/fuse. It is also possible that rabphilin enhances α-actinin-dependent tethering of granules to actin filaments that are directly anchored to the plasma membrane. Such a tether between the granule and the plasma membrane may facilitate subsequent docking/fusion reactions even without dissociation of the vesicle from F-actin. In this respect, we have found that at least some of the granules are clearly connected to the plasma membrane by filaments (Fig. 3). More work is necessary to understand whether such filaments include rabphilin, α-actinin, and actin.

We have shown that α-actinin binds to rabphilin and that interaction of rabphilin with F-actin is α-actinin-dependent. There are four different members of the α-actinin family expressed in mammalian cells (51), skeletal muscle α-actinin-3 and α-actinin-2, which is also expressed in brain (52), and non-muscle α-actinin-1 and -4. In the future it will be interesting to determine whether rabphilin binding to F-actin requires a specific member of the α-actinin family and whether a specific isoform of the α-actinin family localizes to the granule membrane.

Interestingly, it has been recently proposed that synapsins, a family of phosphoproteins that bind both to synaptic vesicles and to the actin cytoskeleton (for review see Ref. 53), also bind to Rab3A (54, 55), raising the possibility that rabphilin/α-actinin and synapsins have similar functions. Other Rab3-binding proteins that are expressed in endocrine cells may also interact with actin cytoskeleton components to regulate granule interactions at the cell cortex. For example, Noc2 (reviewed in Ref. 56), a Rab3-binding protein involved in granule release (57, 58), has been reported to interact with Zyxin, a cytoskeleton component that binds to α-actinin (59).

In conclusion, in this report we have shown that rabphilin binds to the actin cytoskeleton and stimulates *in vitro* binding of granules to cross-linked F-actin structures generated by α-actinin. More work is necessary to understand the role of rabphilin/α-actinin and other Rab3-binding proteins in the positioning of vesicles within F-actin networks.

Acknowledgments—We thank Dr. Brian Storrie for critically reading the manuscript and for helpful discussions. We thank Dr. D. Koticha for preparing the POMC-pEGFP plasmid, Dr. P. De Camilli for rabphilin-pcDNA3, Dr. G. Thomas for POMC-pSP65, Dr. R. Regazzi for Myc-tagged Rab3B cDNA, and Dr. F. Bartolini and Dr. J. Schmoranzer for help with fluorescence microscopy. We thank Sudhindra Swamy and Theresa Swayne of the Confocal Microscopy Facility of the Herbert Irving Comprehensive Cancer Center at the Columbia Presbyterian Medical Center for helping us with the confocal microscope.

REFERENCES

1. Gonzalez, L., Jr., and Scheller, R. H. (1999) *Cell* **96,** 755–758
2. Li, C., Takei, K., Geppert, M., Daniell, L., Stenius, K., Chapman, E. R., Jahn, R., De Camilli, P., and Sudhof, T. C. (1994) *Neuron* **13,** 885–898
3. Iezzi, M., Escher, G., Meda, P., Charollais, A., Baldini, G., Darchen, F., Wollheim, C. B., and Regazzi, R. (1999) *Mol. Endocrinol.* **13,** 202–212
4. Martelli, A. M., Baldini, G., Tabellini, G., Koticha, D. D., Bareggi, R., and Baldini, G. (2000) *Traffic* **1,** 976–986
5. Darchen, F., Senyshyn, J., Brondyk, W. H., Taatjes, D. J., Holz, R. W., Henry, J. P., Denizot, J. P., and Macara, I. G. (1995) *J. Cell Sci.* **108,** 1639–1649
6. Yamaguchi, T., Shirataki, H., Kishida, S., Miyazaki, M., Nishikawa, J., Wada, K., Numata, S., Kaibuchi, K., and Takai, Y. (1993) *J. Biol. Chem.* **268,** 27164–27170
7. Ostermeier, C., and Brunger, A. T. (1999) *Cell* **96,** 363–374
8. Chung, S. H., Joberty, G., Gelino, E. A., Macara, I. G., and Holz, R. W. (1999) *J. Biol. Chem.* **274,** 18113–18120
9. Ubach, J., Garcia, J., Nittler, M. P., Sudhof, T. C., and Rizo, J. (1999) *Nat. Cell Biol.* **1,** 106–112
10. Chung, S. H., Takai, Y., and Holz, R. W. (1995) *J. Biol. Chem.* **270,** 16714–16718
11. Arribas, M., Regazzi, R., Garcia, E., Wollheim, C. B., and De Camilli, P. (1997) *Eur. J. Cell Biol.* **74,** 209–216
12. Nonet, M. L., Staunton, J. E., Kilgard, M. P., Fergestad, T., Hartwieg, E., Horvitz, H. R., Jorgensen, E. M., and Meyer, B. J. (1997) *J. Neurosci.* **17,** 8061–8073
13. Schluter, O. M., Schnell, E., Verhage, M., Tzonopoulos, T., Nicoll, R. A., Janz, R., Malenka, R. C., Geppert, M., and Sudhof, T. C. (1999) *J. Neurosci.* **19,** 5834–5846
14. Stahl, B., Chou, J. H., Li, C., Sudhof, T. C., and Jahn, R. (1996) *EMBO Eur. Mol. Biol. Organ. J.* **15,** 1799–1809
15. Joberty, G., Stabila, P. F., Coppola, T., Macara, I. G., and Regazzi, R. (1999) *J. Cell Sci.* **112,** 3579–3587
16. Staunton, J., Ganetzky, B., and Nonet, M. L. (2001) *J. Neurosci.* **21,** 9255–9264
17. Geppert, M., Bolshakov, V. Y., Siegelbaum, S. A., Takei, K., De Camilli, P., Hammer, R. E., and Sudhof, T. C. (1994) *Nature* **369,** 493–497
18. Zhao, S., Torii, S., Yokota-Hashimoto, H., Takeuchi, T., and Izumi, T. (2002) *Endocrinology* **143,** 1817–1824
19. Waselle, L., Coppola, T., Fukuda, M., Iezzi, M., El-Amraoui, A., Petit, C., and Regazzi, R. (2003) *Mol. Biol. Cell* **14,** 4103–4113
20. Fukuda, M., Kanno, E., and Yamamoto, A. (2004) *J. Biol. Chem.* **279,** 13065–13075
21. Kato, M., Sasaki, T., Ohya, T., Nakanishi, H., Nishioka, H., Imamura, M., and Takai, Y. (1996) *J. Biol. Chem.* **271,** 31775–31778
22. Coppola, T., Hirling, H., Perret-Menoud, V., Gattesco, S., Catsicas, S., Joberty, G., Macara, I. G., and Regazzi, R. (2001) *J. Cell Sci.* **114,** 1757–1764
23. Djinovic-Carugo, K., Young, P., Gautel, M., and Saraste, M. (1999) *Cell* **98,** 537–546
24. Jockusch, B. M., Burger, M. M., DaPrada, M., Richards, J. G., Chaponnier, C., and Gabbiani, G. (1977) *Nature* **270,** 628–629
25. Bader, M. F., and Aunis, D. (1983) *Neuroscience* **8,** 165–181
26. Nakata, T., and Hirokawa, N. (1992) *J. Neurosci.* **12,** 2186–2197
27. Rudolf, R., Salm, T., Rustom, A., and Gerdes, H. H. (2001) *Mol. Biol. Cell* **12,** 1353–1365
28. Baldini, G., Baldini, G., Wang, G., Weber, M., Zweyer, M., Bareggi, R., Witkin, J. W., and Martelli, A. M. (1998) *J. Cell Biol.* **140,** 305–313
29. Benfenati, F., Valtorta, F., Chieregatti, E., and Greengard, P. (1992) *Neuron* **8,** 377–386
30. McKiernan, C. J., Stabila, P. F., and Macara, I. G. (1996) *Mol. Cell Biol.* **16,** 4985–4995
31. Nakano, K., Imai, J., Arai, R., Toh, E. A., Matsui, Y., and Mabuchi, I. (2002) *J. Cell Sci.* **115,** 4629–4639
32. Koticha, D. D., McCarthy, E. E., and Baldini, G. (2002) *J. Cell Sci.* **115,** 3341–3351
33. Martys, J. L., Shevell, T., and McGraw, T. E. (1995) *J. Biol. Chem.* **270,** 25976–25984
34. Dautry-Varsat, A., Ciechanover, A., and Lodish, H. F. (1983) *Proc. Natl. Acad. Sci. U. S. A.* **80,** 2258–2262
35. Sottocasa, G. L., Kuylenstierna, B., Ernster, L., and Bergstrand, A. (1967) *J. Cell Biol.* **32,** 415–438

36. Pelletier, O., Pokidysheva, E., Hirst, L. S., Bouxsein, N., Li, Y., and Safinya, C. R. (2003) *Phys. Rev. Lett.* **91,** 148102
37. Coghill, I. D., Brown, S., Cottle, D. L., McGrath, M. J., Robinson, P. A., Nandurkar, H. H., Dyson, J. M., and Mitchell, C. A. (2003) *J. Biol. Chem.* **278,** 24139–24152
38. Shirataki, H., Kaibuchi, K., Sakoda, T., Kishida, S., Yamaguchi, T., Wada, K., Miyazaki, M., and Takai, Y. (1993) *Mol. Cell Biol.* **13,** 2061–2068
39. Fukuda, M. (2005) *J. Biochem.* (*Tokyo*) **137,** 9–16
40. Mizoguchi, A., Yano, Y., Hamaguchi, H., Yanagida, H., Ide, C., Zahraoui, A., Shirataki, H., Sasaki, T., and Takai, Y. (1994) *Biochem. Biophys. Res. Commun.* **202,** 1235–1243
41. Noel, G., Zollinger, L., Laliberte, F., Rassart, E., Crine, P., and Boileau, G. (1989) *J. Neurochem.* **52,** 1050–1057
42. Riboni, L., Prinetti, A., Bassi, R., Caminiti, A., and Tettamanti, G. (1995) *J. Biol. Chem.* **270,** 26868–26875
43. Lang, T., Wacker, I., Wunderlich, I., Rohrbach, A., Giese, G., Soldati, T., and Almers, W. (2000) *Biophys. J.* **78,** 2863–2877
44. Sunshine, C., Francis, S., and Kirk, K. L. (2000) *Exp. Cell Res.* **257,** 1–10
45. Weber, E., Jilling, T., and Kirk, K. L. (1996) *J. Biol. Chem.* **271,** 6963–6971
46. Johns, L. M., Levitan, E. S., Shelden, E. A., Holz, R. W., and Axelrod, D. (2001) *J. Cell Biol.* **153,** 177–190
47. Otey, C. A., Pavalko, F. M., and Burridge, K. (1990) *J. Cell Biol.* **111,** 721–729
48. Wachsstock, D. H., Wilkins, J. A., and Lin, S. (1987) *Biochem. Biophys. Res. Commun.* **146,** 554–560
49. Bader, M. F., Doussau, F., Chasserot-Golaz, S., Vitale, N., and Gasman, S. (2004) *Biochim. Biophys. Acta* **1742,** 37–49
50. Gasman, S., Chasserot-Golaz, S., Malacombe, M., Way, M., and Bader, M. F. (2004) *Mol. Biol. Cell* **15,** 520–531
51. Otey, C. A., and Carpen, O. (2004) *Cell Motil Cytoskeleton* **58,** 104–111
52. Wyszynski, M., Lin, J., Rao, A., Nigh, E., Beggs, A. H., Craig, A. M., and Sheng, M. (1997) *Nature* **385,** 439–442
53. Greengard, P., Valtorta, F., Czernik, A. J., and Benfenati, F. (1993) *Science* **259,** 780–785
54. Giovedi, S., Vaccaro, P., Valtorta, F., Darchen, F., Greengard, P., Cesareni, G., and Benfenati, F. (2004) *J. Biol. Chem.* **279,** 43760–43768
55. Giovedi, S., Darchen, F., Valtorta, F., Greengard, P., and Benfenati, F. (2004) *J. Biol. Chem.* **279,** 43769–43779
56. Cheviet, S., Waselle, L., and Regazzi, R. (2004) *Trends Cell Biol.* **14,** 525–528
57. Haynes, L. P., Evans, G. J., Morgan, A., and Burgoyne, R. D. (2001) *J. Biol. Chem.* **276,** 9726–9732
58. Manabe, S., Nishimura, N., Yamamoto, Y., Kitamura, H., Morimoto, S., Imai, M., Nagahiro, S., Seino, S., and Sasaki, T. (2004) *Biochem. Biophys. Res. Commun.* **316,** 218–225
59. Crawford, A. W., Michelsen, J. W., and Beckerle, M. C. (1992) *J. Cell Biol.* **116,** 1381–1393

Rabphilin Localizes with the Cell Actin Cytoskeleton and Stimulates Association of Granules with F-actin Cross-linked by α-Actinin

Giovanna Baldini, Alberto M. Martelli, Giovanna Tabellini, Chad Horn, Khaled Machaca, Paola Narducci and Giulia Baldini

J. Biol. Chem. 2005, 280:34974-34984.
doi: 10.1074/jbc.M502695200 originally published online July 25, 2005
